BUTTERWORTH HEINEMANN

Polymer Vol. 36 No. 13, pp. 2553–2558, 1995
Copyright © 1995 Elsevier Science Ltd
Printed in Great Britain. All rights reserved
0032-3861/95/$10.00+0.00

Effect of the heterogeneous distribution of lamellar stacks on amorphous relaxations in semicrystalline polymers

Bryan B. Sauer* and Benjamin S. Hsiao
E.I. du Pont de Nemours and Company Inc., Central Research and Development, Experimental Station, Wilmington, DE 19880, USA
(Received 1 August 1994)

Polymers crystallized at high temperatures, such as poly(aryl ether ether ketone) (PEEK), poly(ethylene terephthalate) and a thermoplastic polyimide, exhibit well developed lamellar stacks. We have obtained small angle X-ray scattering (SAXS) and wide angle X-ray diffraction data at 290°C and 25°C for PEEK and have also utilized literature SAXS data taken at 25°C for the other materials. To model these systems we assume that the interlamellar 'amorphous' or non-crystalline species do not contribute to the glass transition and use the SAXS parameters to calculate a total rigid fraction. Using this assumption it is shown that we can qualitatively describe the strength of glass transitions measured directly by thermal analysis. No other rigid 'amorphous' fractions (RAFs) are needed to model the data under these crystallization conditions. The results suggest that conventionally measured glass transitions originate from the broad amorphous gaps between lamellar stacks in these space-filling spherulitic systems. In situations of very high crystallinities or systems with other crystal morphologies such as defective or high surface area lamellar stack morphologies, the model does not work and the conventional analysis assuming an RAF associated with crystal surfaces is more appropriate.

(Keywords: lamellar stacks; amorphous relaxations; semicrystalline polymers)

INTRODUCTION

The failure of the ideal two-phase model for semicrystalline polymer morphology has been recognized for a few decades. A modified two-phase model was first used to interpret thermal analysis results of relaxations in highly crystalline poly(oxymethylene) (POM)[1], and subsequently applied to many other polymers. The total 'rigid fraction' ($f_r^{d.s.c.}$) determined directly by differential scanning calorimetry (d.s.c.), consisting of both crystalline and 'rigid' amorphous species, was extracted from the calorimetric data taken around the glass transition[1]

$$f_r^{d.s.c.} = 1 - \Delta C_p/\Delta C_p^{amorph} \quad (1)$$

Here, ΔC_p is the change in heat capacity across the glass transition for the semicrystalline polymer, and ΔC_p^{amorph} is the change in heat capacity for the amorphous polymer. By using an independently measured bulk volume fraction crystallinity (W_c), this modified two-phase model allows one to estimate the rigid 'amorphous' fraction (RAF)[1-4]

$$RAF = (1 - \Delta C_p/\Delta C_p^{amorph}) - W_c \quad (2)$$

The RAF is suggested to consist of 'amorphous' or non-crystalline material highly constrained because of its close proximity to crystallite surfaces[3,5]. This is highly dependent on the type of polymer and the crystal morphology. For example, Cheng *et al.*[3] have shown that at a constant level of crystallinity in poly(aryl ether ether ketone) (PEEK), more defective, high surface area crystal morphologies lead to a much larger RAF than those for well developed lamellar crystals.

Extensive calorimetric studies of the magnitude of the glass transition indicated that no 'relaxation' of the RAF in POM occurred up to the melting point[1]. Relaxation of the RAF in poly(aryl ether ether ketone)[3] was also not observed at temperatures well above the nominal T_g, while the RAF for polypropylene continuously decreased with increasing temperature above the nominal T_g until it became zero just before the melting point[2]. Loufakis and Wunderlich[4] also showed that with some even more flexible semicrystalline polymers, the RAF could not be detected. However, with 'stiff' polymers, the presence of constrained amorphous species is a general feature[1-11].

Small angle X-ray scattering (SAXS) analysis[12] has shown that the ideal two-phase model for some well crystallized semicrystalline polymers is insufficient[13]. Consider a space-filling spherulitic system such as in the top of *Figure 1*, where the spherulites are impinged. SAXS results[13] show that many of these space-filling spherulitic systems are inhomogeneously filled with dense crystalline lamellar stacks or fibrils[14] consisting of approximately three to 10 lamellar sheets separated by broad non-crystalline gaps (*Figure 1*, middle). Generally, the coherently scattering lamellar stacks are ca. 70% crystalline[13], while the bulk crystallinity is less than 40% (*Table 1*)! This emphasizes the fact that it is

* To whom correspondence should be addressed

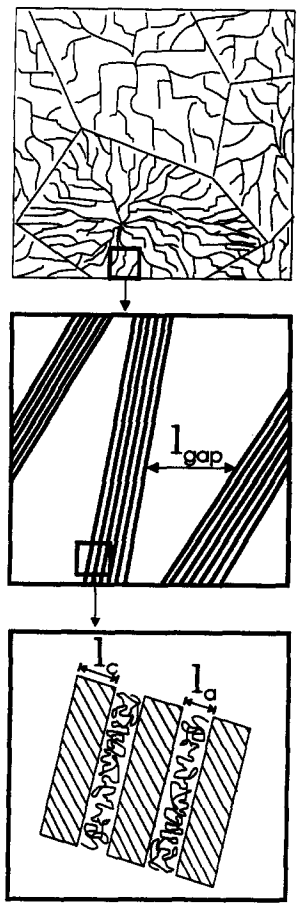

Figure 1 Schematic illustrating a space-filling spherulitic system with heterogeneously distributed lamellar stacks: (top) schematic of the morphology of impinged spherulites; (middle) heterogeneously distributed lamellar stacks separated by a broad amorphous gap; (bottom) lamellar crystal thicknesses (l_c) and interlamellar non-crystalline (l_a) thickness within a stack

Table 1 Calculated rigid fractions based on room temperature SAXS data and d.s.c. data[a]

	PEEK	N-TPI	PET	PET
T_c (°C)	300 (2 h)	310 (3 h)	240 (9 h)	190 (1 h)
W_c	0.37	0.36	0.46	0.36
L	12.7	17.0	10.8	10.0
l_c	9.3	12.1	7.6	6.5
l_a	3.4	4.9	3.2	3.5
$f_r^{d.s.c.} = 1 - \Delta C_p/\Delta C_p^{amorph}$	0.47[b]	0.50[c]	0.63[c]	0.72[c]
$RAF = f_r^{d.s.c.} - W_c$	0.10[d]	0.11[d]	0.22[d]	0.36[d]
$f_r^{SAXS} = W_c(1 + l_a/l_c)$	0.50[e]	0.51[c]	0.65[f]	0.56[f]
$f_r^{d.s.c.} - f_r^{SAXS}$	−0.03	−0.01	−0.02	0.16
l_{gap}	62[g]	83[g]	28[g]	40[g]

[a] All lengths are in nanometres. Bulk volume fraction crystallinities (W_c) were generally determined from the density. T_c, crystallization temperature; L, long period; l_c, lamellar thickness, l_a, interlamellar amorphous thickness
[b] From Cheng *et al.*[3]
[c] From this work
[d] See equation (2)
[e] From Hsiao and Sauer[15]
[f] From Santa Cruz *et al.*[13]
[g] Calculated using eqn (4) by assuming on average that there are five lamellae per stack. The calculated value for the amorphous gap between stacks (l_{gap}) is not extremely sensitive to this assumption

erroneous to use the Bragg spacing and the bulk degree of crystallinity to calculate the lamellar thicknesses. This procedure results in abnormally thin lamellar dimensions. Instead, one must use the linear degree of crystallinity (i.e. ca. 70%) determined from the appropriate analysis of SAXS data[13]. Transmission electron microscopy (TEM) results support the lamellar stack morphology, especially for high temperature crystallization conditions[14,16]. These specific morphologies will be key factors in allowing us to model amorphous relaxations in the systems studied here.

Unlike many semicrystalline polymers such as PEEK and poly(ethylene terephthalate) (PET) where T_g is only shifted upwards by a few degrees compared to the purely amorphous material, in semicrystalline poly(butylene terephthalate) (PBT)[6] the constraining effect of the crystal surfaces increases T_g by ca. 65°C above the original amorphous T_g. At first glance this is surprising, since PBT is relatively flexible and has a relatively large interlamellar non-crystalline layer thickness (l_a) of 8 nm by SAXS[17]. It is also approximately lamellar space filling, i.e. all non-crystalline material is constrained between lamellae. PBT can be contrasted with the 'stiff' chain nature of the polymers studied here and the very narrow interlamellar non-crystalline layer thicknesses (e.g. $l_a = 2-5$ nm in PET[13] and similar dimensions in PEEK and N-TPI (*Table 1*)). It is thus logical to apply a model which assumes that the species in these very narrow gaps are 'completely constrained', i.e. they do not relax until one approaches the melting point[3]. The species which do contribute to the glass transition are likely to be those in the broad amorphous gaps between lamellar stacks which are of the order of l_{gap}, ca. 10–100 nm (*Figure 1* and *Table 1*). These broad gaps explain why the commonly measured T_g values in semicrystalline PEEK, PET and other related polymers are not shifted to significantly higher temperatures.

In addition to PBT, another flexible polymer which has been widely studied is linear polyethylene (PE). For moderate to low molecular weights (MWs), any RAF detectable by calorimetric methods is relaxed by ca. −20°C, which is roughly the upper limit of the very broad glass transition[1,18,19]. Other techniques such as Raman internal and longitudinal acoustic modes (LAMs)[20] and n.m.r.[21] show that the crystal/amorphous interfacial fraction in PE is small at moderate MWs (< ca. 50 000 g mol^{-1}), yet increases continuously as the MW is increased[20,21]. Calorimetry data also show some unusual behaviour for ultrahigh MW PE (> ca. 3000 000 g mol^{-1}) in the glass transition region[19] consistent with a broader interfacial region. The broad interfacial region is suggested to arise because of the decreased mobility in ultrahigh MW PE[20]. Even though PE is flexible, for ultrahigh MW PE it is suggested[19] that this interfacial region can be related to an RAF such as that detected in other polymers such as POM[1], but smaller in magnitude.

In our preliminary report[22] we made the assumption that the interlamellar non-crystalline species are rigid or completely constrained. This assumption allows one to derive equation (3) in order to predict the total rigid fraction (f_r^{SAXS}) from SAXS parameters and independently measured values of the bulk volume fraction crystallinity W_c

$$f_r^{SAXS} = W_c(1 + l_a/l_c) \quad (3)$$

Here, l_c is the lamellar crystal thickness and l_a is the interlamellar 'amorphous' or non-crystalline layer thickness calculated from SAXS data. Note that f_r^{SAXS} is the *total* volume fraction of non-crystalline plus

crystalline material *within* the lamellar stacks, and includes no other rigid amorphous phase. The directly measured total rigid fraction $f_r^{d.s.c.} = 1 - \Delta C_p/\Delta C_p^{amorph}$ can be compared with f_r^{SAXS} in order to test the model. At this point we summarize the specific conditions for which one can expect this approach to be justified.

1. The polymers are crystallized at relatively high temperatures in order to develop and perfect the lamellar stack morphology. We are not considering lower temperature crystallization conditions which may lead to defective, high surface area crystallites and stacks.
2. Polymers are spherulitically space filling. Crystallization is essentially complete and does not change as the sample is quenched to 25°C, as is indicated by the comparison of wide angle X-ray diffraction (WAXD) and SAXS data at high and low temperatures on the same precrystallized sample (see below).
3. The polymers in question are generally moderate in crystallinity ($W_c <$ ca. 50%).
4. Homogeneous lamellar space-filling 'flexible' polymers such as polyethylene[23] and PBT[17] are not considered. Also, these generally do not have small l_a values[17,23].

EXPERIMENTAL

The thermoplastic polyimide N-TPI (from Mitsui-Toatsu Chemicals) was made from 4,4′-bis(3-aminophenoxy)biphenyl and pyromellitic dianhydride (PMDA); it has a T_g of ca. 250°C and an apparent melting point of ca. 385°C[24]. PET was obtained from Scientific Polymer Products (Ontario, NY) and had a weight average MW of 45 000 g mol^{-1}. PEEK 150G was obtained from ICI.

The simultaneous SAXS/WAXD data were obtained with the X3A2 SUNY beamline at the National Synchrotron Light Source, Brookhaven National Laboratory ($\lambda = 0.154$ nm) using a dual-chamber temperature jump device[25] and two linear position sensitive Braun detectors. A typical data collection time for each pattern was 30 s.

Accurate percentage crystallinities were difficult to obtain and crucial for our analysis. We have found that the room temperature density method is the most reliable one to obtain the percentage crystallinity. Volume fraction crystallinities W_c were determined using amorphous and crystal densities of 1.263 g cm^{-3} and 1.40 g cm^{-3}, respectively[15]. WAXD crystallinity indices converted to volume percentage crystallinities were more qualitative but consistent with our 25°C density determinations (*Table 2*). There is still some controversy as to the proper method for estimation of the percentage crystallinity by d.s.c.[11]. Some evidence indicates that proper analysis of the heat of fusion will also generally lead to accurate percentage crystallinities consistent with those determined by the density method[11].

RESULTS

All data for N-TPI were measured in this laboratory and the SAXS data were reported previously[26]. The SAXS data for PET were taken from the literature[13], and d.s.c. measurements of the change in heat capacity at the glass transition (ΔC_p) were made in our laboratory. The magnitude of ΔC_p was analysed following the method of Grebowicz *et al.*[2]. All samples were crystallized at the temperatures indicated in *Table 1* in an N_2-purged vacuum oven under conditions where significant degradation would not occur. Typical d.s.c. results for amorphous and crystallized N-TPI and PET samples are shown in *Figures 2* and *3*, respectively. The values of ΔC_p are given in the figure captions. In *Table 1*, some d.s.c. data[3], SAXS data[15] and bulk crystallinity data[15] were taken from the literature for PEEK (grade 150G from ICI). These are summarized for the 300°C-crystallized PEEK sample in *Table 1*.

Table 2 Lamellar variables calculated by SAXS correlation function analysis for PEEK crystallized at 290°C for 24 h with subsequent SAXS/WAXD measurements at 290°C and 25°C[a]

	290°C	25°C
Density (g cm^{-3})		1.308
W_c (density)	0.34[b]	0.34 (25°C)[b]
W_c (WAXD)[c]	0.33 ± 0.02 (290°C)	0.33 ± 0.02 (25°C)
Q[d]	9.7	9.7
L	13.0	12.1
l_c	8.7 ± 0.5	8.0 ± 0.5
l_a	4.3 ± 0.3	4.1 ± 0.3
$f_r^{d.s.c.} = 1 - \Delta C_p/\Delta C_p^{amorph}$	0.54	0.54
$RAF = f_r^{d.s.c.} - W_c$	0.20	0.20
$f_r^{SAXS} = W_c(1 + l_a/l_c)$	0.51	0.51
$f_r^{d.s.c.} - f_r^{SAXS}$	0.03	0.03

[a] See *Table 1* for some of the definitions
[b] Densities were only measured at room temperature. Volume fraction crystallinities W_c were determined using amorphous and crystal densities of 1.263 g cm^{-3} and 1.40 g cm^{-3}, respectively. For the purpose of calculating f_r^{SAXS}, we assumed the same W_c at high temperatures. This is roughly verified by the WAXD crystallinity index converted to W_c, which was found to be the same within experimental error at 25°C and 290°C
[c] W_c (WAXD) is equal to the WAXD crystallinity index (Ψ) multiplied by ρ/ρ_c (= 1.308/1.4). WAXD was performed at two temperatures
[d] SAXS invariant in arbitrary units

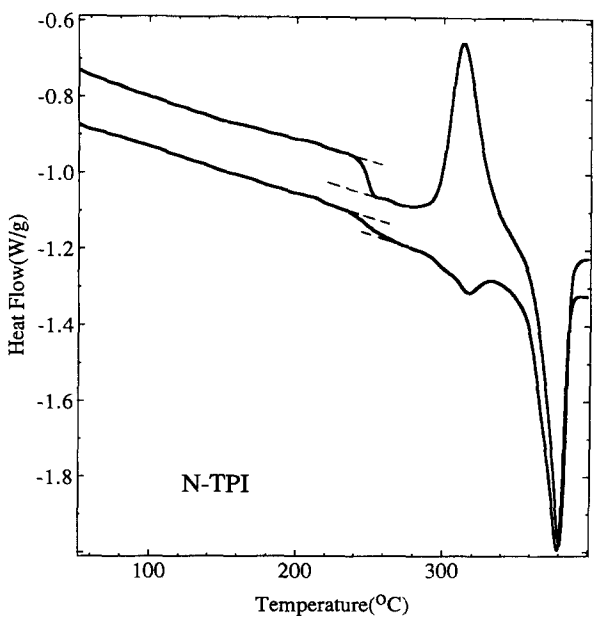

Figure 2 D.s.c. results at a 20°C min^{-1} heating rate for amorphous (upper) and 310°C melt crystallized (lower) N-TPI samples. The values of ΔC_p are 0.094 W g^{-1} and 0.047 W g^{-1}, respectively

Temperature dependent SAXS/WAXD data in addition to the d.s.c. and density-related results in *Table 2* were obtained in this study. The results were obtained in an attempt to address the important question of whether additional crystallinity develops after quenching 'well crystallized' samples to room temperature. For this high temperature study, PEEK was premelted at 390°C for 10 min, melt crystallized by dropping the temperature rapidly to 290°C and holding for 24 h, quenched to room temperature for the simultaneous SAXS/WAXD study, and then heated to 290°C again to obtain simultaneous SAXS/WAXD data on the same sample. WAXD data at 290°C and 25°C are shown in *Figure 4*. The backgrounds, mainly due to the non-crystalline fractions, were subtracted from the raw data to give these results. To estimate the contributions from the non-crystalline fractions at 25°C, a profile of a quenched amorphous sample was used, and at 290°C the profile for an initially molten sample at 290°C was taken from the time dependent WAXD. By taking the ratio of the integrated crystal intensity to the total integrated intensity (crystal plus non-crystalline background), crystallinity indices can be calculated. Because the amorphous background is lower at 290°C, a comparable crystallinity index of about 35% is calculated from this analysis at both temperatures. This is converted to a volume percentage crystallinity and the values are listed in *Table 2*.

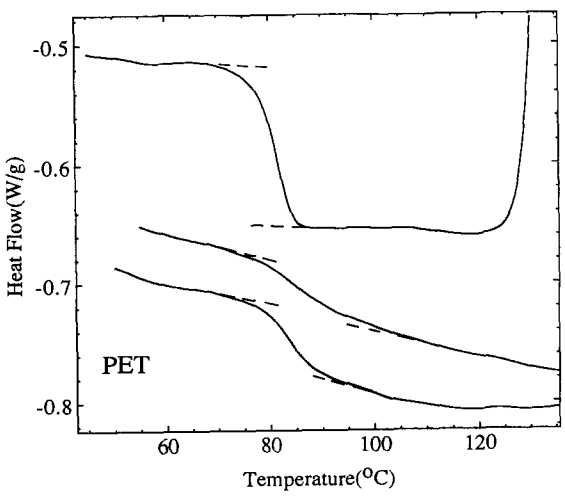

Figure 3 D.s.c. results at 20°C min^{-1} for amorphous (top), 190°C melt crystallized (middle) and 240°C melt crystallized (bottom) PET. The values of ΔC_p are 0.120 W g^{-1}, 0.034 W g^{-1} and 0.044 W g^{-1}, respectively

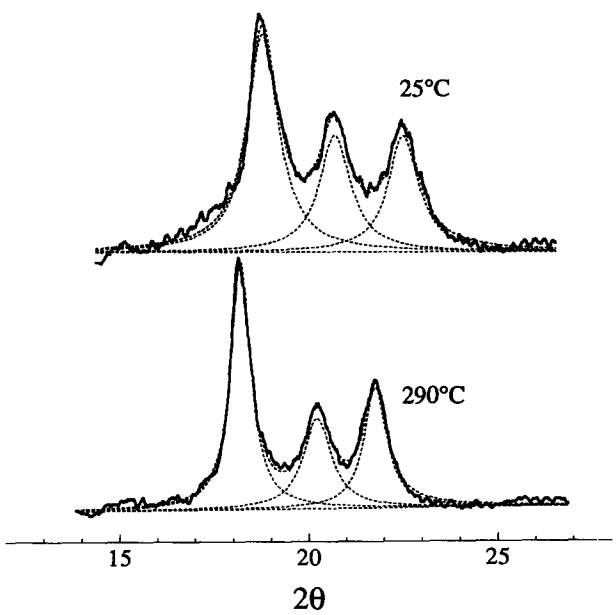

Figure 4 Extracted wide angle X-ray diffraction (WAXD) data of the crystalline component in a PEEK sample precrystallized at 290°C for 24 h. WAXD data were obtained at the two temperatures indicated (see text)

Each crystal diffraction profile was deconvoluted into three Lorentzian peaks indicating the 110, 111 and 200 reflections. It was found that the total integrated intensity decreased by about 25% from 25°C to 290°C. The integral breadths of each of the three reflection peaks also became broader at 25°C, which was expected because of microstrains below T_g which lead to fluctuations in the lattice parameters of the crystals at 25°C[27,28]. The decrease in the integrated intensity of all peaks at 290°C was also expected. There are at least two possible explanations for the decrease in intensity. One is that during the rapid quenching of this highly crystalline sample, a small number of additional imperfect crystals (i.e. <5%) are developed which broaden and intensify the reflection peaks. At high temperatures, these crystals melt away, leading to a reduced intensity and sharper reflection peaks. The SAXS data presented in *Figure 5* show no indication of additional crystallinity in the lamellar region, which is evidence that this may be an incorrect hypothesis. Another explanation, perhaps the more likely one, is that the decreasing intensity of the reflection at high temperature is simply due to thermal vibrations of the molecules in the crystals (thermal vibrations do not change the integral breadth of the reflections)[27,28]. The Debye–Waller factor from enhanced thermal motions at high temperatures is well known to decrease significantly the WAXD reflected intensity of the crystal. For a temperature change from 25°C to 290°C, one could expect a 25–50% decrease.

All three reflection peaks are shifted to lower 2θ values at 290°C in *Figure 4*. These changes are explained by thermal expansion of the unit cell. Detailed analysis using an orthorhombic cell indicates that the a parameter is 7.88 Å (1 Å = 0.1 nm) at 25°C and 8.16 Å at 290°C, the b parameter is 5.89 Å at 25°C and 6.07 Å at 290°C, whereas the c parameter is essentially unchanged with a value of about 9.91 Å. The calculated specific crystal volumes at the two temperatures are consistent with those reported earlier[29]. A total crystal volume change of about 7% is determined from 25°C to 290°C.

The corresponding SAXS profiles are shown in *Figure 5*. In this figure, the 290°C profile is slightly higher in intensity, but the peak position also shifts to a lower q value. We have used the correlation function method (*Figure 5*, bottom) to estimate the morphological parameters of the lamellar stacks from these data, and the results are listed in *Table 2*. It is found that the long period L increases from 12.1 nm to 13.0 nm (by 7%), the lamellar thickness l_c increases from 8.0 nm to 8.7 nm (by 9%) and the interlamellar amorphous thickness l_a increases from 4.1 nm to 4.3 nm (by 5%) when the temperature rises from 25°C to 290°C. All these changes are similar to the volume thermal expansion coefficient

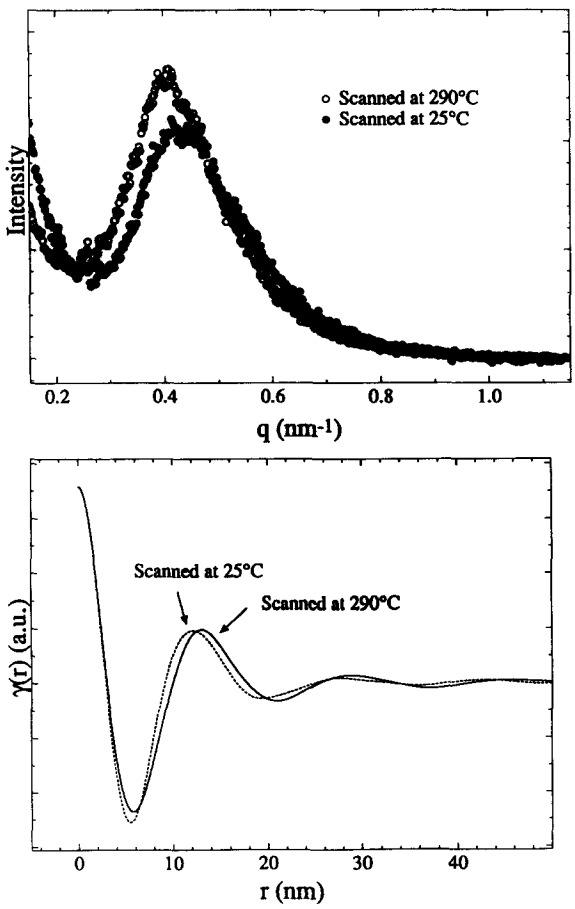

Figure 5 Raw SAXS data (top) and calculated SAXS correlation functions (bottom) for a precrystallized PEEK sample (290°C for 24 h) at the two temperatures indicated (see text). The data were taken simultaneously with the WAXD data in *Figure 4*

measured for the unit cell. The error bars (ca. 8%) are large enough that one cannot reliably ascertain whether the thermal expansions of the crystal or the non-crystalline regions are larger. We conclude from the temperature dependent SAXS results (*Table 2*) that the morphological parameters are essentially the same at high and low temperatures. This, and the fact that the scattering invariants $Q(=\phi_v\phi_a(\rho_c-\rho_a)^2)$ are equal at both temperatures (bottom of *Figure 5* and *Table 2*), suggests that no recrystallization or melting occurs in the lamellar stack regions. The WAXD results discussed above are also consistent with this conclusion.

DISCUSSION

We shall consider only SAXS data analysed using the correlation function method[12,13]. Santa Cruz *et al.*[13] have shown that this gives reliable results for l_a and l_c. More importantly, it was shown that the linear degree of crystallinity (l_c/L, where L is the long period) is relatively independent of the model chosen to fit the SAXS data[13]. Numerically, it is only the model independent ratios such as l_a/l_c, calculated from l_c/L using $l_a + l_c = L$, which are important in our calculations. The data for three polymers under specific crystallization conditions are summarized in *Table 1*. From the agreement of $f_r^{d.s.c.}$ and f_r^{SAXS} for PEEK in *Tables 1* and *2*, it is clear that the heterogeneous lamellar stacks model (equation (3)) qualitatively describes the data. This justifies our assumption (equation (3)) that the interlamellar non-crystalline species cannot contribute to the glass transition. The good agreement between $f_r^{d.s.c.}$ and f_r^{SAXS} indicates that no other RAF is needed to fit the PEEK data within the experimental precision. The high temperature SAXS data (*Table 2*) were taken because of the concern that the SAXS parameters measured at room temperature may not be representative of the morphology probed by the higher temperature d.s.c. determination of ΔC_p in the glass transition region. It is seen that essentially identical results are obtained independent of temperature (*Table 2*), showing that little or no crystallization occurs upon quenching. The majority of the observed changes in the SAXS/WAXD parameters with temperature are due to thermal expansion, as was discussed above.

The same agreement between $f_r^{d.s.c.}$ and f_r^{SAXS} is seen for N-TPI crystallized at 310°C and PET crystallized at 240°C (*Table 1*), presumably because the lamellar stacks are relatively well developed, and because the amorphous gaps (l_{gap}) between stacks are rather large, so that any RAF other than the interlamellar non-crystalline rigid fraction contributes negligibly.

It is important to contrast some of these results with those for lamellar space-filling systems such as PBT and PE. As was discussed earlier, in semicrystalline PBT compared to amorphous PBT, T_g is shifted upwards by a surprisingly large value of ca. 65°C, even though PBT is quite 'flexible' and has a rather large l_a of 8 nm[17]. In PBT, the stacks are essentially space filling and all the non-crystalline material is between lamellae. One hypothesis is that there is a continuous spectrum of constrained material as one traverses the interlamellar non-crystalline layer. The broad and shifted glass transitions in semicrystalline PBT and PE are good evidence for this continuous spectrum of species with differing degrees of constraint. Suitable techniques for quantification are n.m.r.[21] and Raman LAM[20], which allow one to divide this continuous spectrum into roughly two separate fractions: mobile and rigid amorphous. Presumably, the more 'rigid' non-crystalline species are closest to the crystal surfaces. For lamellar space-filling systems such as PBT, equation (3) is not valid and the standard methodology using equation (2) is appropriate, showing that one can readily detect a large RAF under all crystallization conditions[6].

Data for a low temperature crystallized PET sample are given as a counter example in *Table 1* for a case where one would expect equation (3) to fail. The rigid fraction determined by d.s.c., $f_r^{d.s.c.}$ is significantly larger than f_r^{SAXS} (0.72 vs. 0.56). There are two likely reasons for this difference. Because of the high nucleation density, it is likely that some crystals exist which are not associated with lamellar stacks, and the constrained non-crystalline species associated with them would contribute to $f_r^{d.s.c.}$ but not to f_r^{SAXS}. The same effect would arise from any defective and high surface area stacks. Thus, $f_r^{d.s.c.} - f_r^{SAXS}$ for 190°C-crystallized PET is quite large because of the RAF associated with these non-periodic crystallite surfaces. These contributions are not accounted for by equation (3). Many other examples of low temperature or non-isothermally crystallized samples exhibit this type of behaviour because of the presence of high surface area and ill-developed lamellar

stacks[3,9]. A final technical issue regards the SAXS data analysis. For low temperature crystallized samples such as 190°C-crystallized PET, the weak and diffuse SAXS data from defective lamellar stacks are difficult to analyse accurately, and this could lead to other errors in any model predictions.

In *Table 1*, the calculated dimensions of the amorphous gaps (as defined in *Figure 1*) between lamellar stacks (l_{gap}) are given. These are estimated using geometric arguments

$$W_c = \frac{5l_c}{5l_c + 5l_a + l_{gap}} \quad (4)$$

Here we have assumed that there are five lamellae per stack[13]. The calculated values of l_{gap} are not too sensitive to the assumed number of lamellae per stack, as long as this is roughly in the region of three to 10. Because these amorphous gaps are broad, the species contained within them are not significantly constrained by the crystallite surfaces, and T_g does not increase significantly in these systems (e.g. *Figures 2* and *3*). It should also be noted that l_{gap} is not relevant for polymers such as PBT where the lamellar stacks are homogeneously space filling.

CONCLUSIONS

In systems such as PEEK, PET and N-TPI crystallized at high temperatures, l_a is small. We have obtained SAXS/WAXD data at 290°C and 25°C for PEEK and have also utilized literature SAXS data taken at 25°C for the other materials. To model these systems we assumed that the interlamellar 'amorphous' or non-crystalline species do not contribute to the glass transition, and used the SAXS parameters to calculate a total rigid fraction. This assumption allows one to describe qualitatively the strength of glass transitions measured directly by thermal analysis. This applies only to certain polymers crystallized at high temperatures where lamellar stacks are well developed. No other rigid 'amorphous' fractions are needed to model the data under these crystallization conditions. The results suggest that conventionally measured glass transitions originate from the broad amorphous gaps between lamellar stacks in these space-filling spherulitic systems. In situations of very high crystallinities or systems with other crystal morphologies such as defective or high surface area lamellar stack morphologies, the model does not work and the conventional analysis assuming an RAF associated with crystal surfaces is more appropriate. Besides improving our general understanding of the origin of amorphous relaxations, the model also has important implications for semicrystalline polymers with regard to diffusion, phase morphology in blends and oriented systems, and the basic interpretation of thermal analysis data.

ACKNOWLEDGEMENTS

We thank our Du Pont colleagues including Dr Richard Ikeda for helpful discussions and Nicholas DiPaolo, Joe McKeown and William Kampert for their experimental work.

REFERENCES

1 Suzuki, H., Grebowicz, J. and Wunderlich, B. *Makromol. Chem.* 1985, **186,** 1119
2 Grebowicz, J., Lau, S. F. and Wunderlich, B. *J. Polym. Sci., Polym. Phys. Edn* 1984, **71,** 19
3 Cheng, S. Z. D., Cao, M.-Y. and Wunderlich, B. *Macromolecules* 1986, **19,** 1868
4 Loufakis, K. and Wunderlich, B. *Macromolecules* 1987, **20,** 2474
5 Huo, P. and Cebe, P. *Macromolecules* 1992, **25,** 902
6 Cheng, S. Z. D., Pan, R. and Wunderlich, B. *Makromol. Chem.* 1988, **189,** 2443
7 Cheng, S. Z. D. and Wunderlich, B. *Macromolecules* 1987, **20,** 1630
8 Cheng, S. Z. D. and Wunderlich, B. *Macromolecules* 1987, **20,** 2802
9 Huo, P. and Cebe, P. *Colloid Polym. Sci.* 1992, **270,** 840
10 Huo, P. and Cebe, P. *Polymer* 1993, **34,** 696
11 Velikov, V., Vivirito, J., Verma, R. K. and Marand, H. *Macromolecules* 1995, in press
12 Strobl, G. R. and Schneider, M. *J. Polym. Sci., Polym. Phys. Edn* 1980, **18,** 1343
13 Santa Cruz, C., Stribeck, N., Zachmann, H. G. and Balta Calleja, F. J. *Macromolecules* 1991, **24,** 5980
14 Lovinger, A. J., Hudson, S. D. and Davis, D. D. *Macromolecules* 1992, **25,** 1752
15 Hsiao, B. S. and Sauer, B. B. *J. Polym. Sci., Polym. Phys. Edn* 1993, **31,** 901
16 Groeninckx, G., Reynaers, H., Berghmans, H. and Smets, G. *J. Polym. Sci.* 1980, **18,** 1311
17 Runt, J. P., Zhang, X., Miley, D. M., Gallagher, K. P. and Zhang, A. *Macromolecules* 1992, **25,** 3902
18 Gaur, U. and Wunderlich, B. *Macromolecules* 1980, **13,** 445
19 Gaur, U. and Wunderlich, B. *J. Phys. Chem. Ref. Data* 1981, **10,** 119
20 Mandelkern, L., Alamo, R. G. and Kennedy, M. A. *Macromolecules* 1990, **23,** 4721
21 Kitamaru, R., Horii, F. and Murayama, K. *Macromolecules* 1986, **19,** 636
22 Sauer, B. B. and Hsiao, B. S. *Am. Chem. Soc. Prepr., Polym. Mater. Sci. Eng.* 1993, **69,** 35
23 Voigt-Martin, I. G. and Mandelkern, L. *J. Polym. Sci., Polym. Phys. Edn* 1984, **22,** 1901
24 Hou, T. H. and Reddy, R. M. *SAMPE Q.* 1991, **22,** 38
25 Song, H. H., Wu, D. Q., Chu, B., Satkowski, M., Ree, M., Stein, R. S. and Phillips, J. C. *Macromolecules* 1990, **23,** 2380
26 Hsiao, B. S., Sauer, B. B. and Biswas, A. *J. Polym. Sci., Polym. Phys. Edn* 1994, **32,** 737
27 Hosemann, R. and Bagchi, S. N. 'Direct Analysis of Diffraction by Matter', North-Holland, Amsterdam, 1962
28 Balta-Calleja, F. J. and Vonk, C. G. 'X-ray Scattering of Synthetic Polymers', Elsevier, New York, 1989, Ch. 4
29 Zoller, P., Kehl, T. A., Starkweather, H. W. and Jones, G. *J. Polym. Sci., Polym. Phys. Edn* 1989, **27,** 993